Facile Propeller Rotation in Metallacyclopropanes. Synthesis and Dynamic Behavior of New Tetrafluoroethylene–Ruthenium Complexes. Crystal and Molecular Structure of $[Ru(\eta^5\text{-}C_5Me_5)Cl(\eta^2\text{-}C_2F_4)]_2$

Owen J. Curnow,[1a] Russell P. Hughes,*[,1a] Erin N. Mairs,[1a] and Arnold L. Rheingold[1b]

Departments of Chemistry, Burke Chemistry Laboratory, Dartmouth College, Hanover, New Hampshire 03755-3564, and University of Delaware, Newark, Delaware 19716

Received March 12, 1993

Reaction of the tetramer $[RuCp^*Cl]_4$ ($Cp^* = C_5Me_5$) with tetrafluoroethylene gives the sparingly soluble dimer $[RuCp^*(C_2F_4)Cl]_2$ (**3**), the molecular structure of which has been determined by a single crystal X-ray diffraction study. Crystal data for **3**: monoclinic, space group $P2_1/n$; $Z = 2$; $a = 8.059(2)$ Å, $b = 20.504(6)$ Å, $c = 8.830(1)$ Å, $\beta = 116.28(1)°$; $V = 1308.3(5)$ Å^3; $T = 298$ K; $R = 0.0456$; $R_w = 0.0530$ based on 2461 reflections for $F_o \geq n\sigma(F_o)$ ($n = 0$). Reaction of this dimer with a neutral donor ligand L gives soluble monomeric complexes $[RuCp^*(C_2F_4)(L)Cl]$ (**5a–d** L = PMe_3, $P(OMe)_3$, pyridine, *t*-BuNC), while reaction with anionic chelating ligands LX^- gives soluble monomers $[RuCp^*(C_2F_4)(LX)]$ (**6a,b** LX = 8-hydroxyquinolinato, 8-hydroxyquinaldinato; **4a–c** LX = acetylacetonato, trifluoroacetylacetonato, 2,6-dimethylheptane-3,5-dionato). Despite having metallacyclopropane structures that are usually associated with high barriers to propeller rotation, variable temperature ^{19}F-NMR spectra of the soluble tetrafluoroethylene complexes **4–6** reveal unprecedently low barriers to propeller rotation of the C_2F_4 ligand about the Ru–olefin axis. A series of free energies of activation ($\Delta G^\ddagger$) for propeller rotation have been measured. The observed low barriers are explained by considering the [RuCp*LX] fragment, to a first order approximation, as an ML_5 fragment with filled, orthogonal, and almost degenerate orbitals available on the Ru fragment for π back-bonding with the olefin.

Introduction

Transition metal–olefin complexes have been extensively studied since the structural characterization of Zeise's salt.[2] Their role in several catalytic processes, including olefin hydrogenations, hydroformylations, isomerizations, oxidations, and polymerizations, is testament to their importance as organometallic reagents and intermediates.[3] It is generally accepted that the best way of describing the transition metal–olefin interaction is the two-component interaction, originally proposed by Dewar, Chatt, and Duncanson,[4] involving an olefin π to metal d σ-bonding interaction and a metal d to olefin π^* π-bonding interaction (Figure 1).

There has been considerable work done on the experimental measurement and theoretical prediction of the activation barriers to propeller rotation of the olefin about the metal–olefin bond axis so as to understand the nature of the metal–olefin interaction.[5] Also, propeller rotation is usually necessary for olefin insertion reactions, a basic step in most catalytic processes involving olefins,[3] as a means of achieving the particular orientation required for insertion. This requirement is not generally a problem because olefin rotation is almost always much more facile than olefin insertion.[3] While the σ-bonding interaction (Figure 1A) is cylindrically symmetric and cannot, therefore, lead to any barrier to propeller rotation, it is the

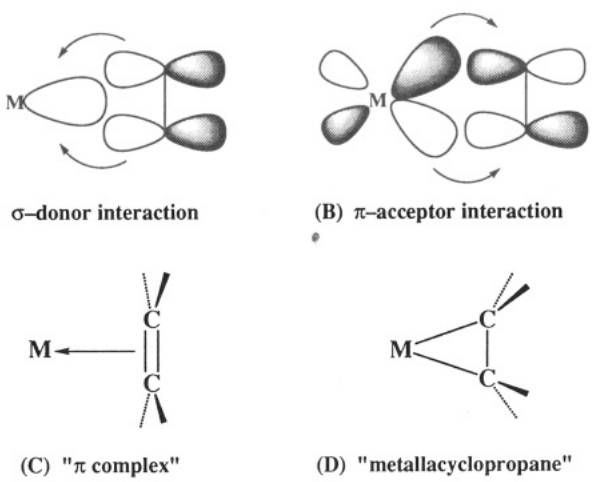

(A) σ–donor interaction (B) π–acceptor interaction

(C) "π complex" (D) "metallacyclopropane"

Figure 1. Components of the transition metal–olefin interaction [(A) σ-donor and (B) π-acceptor] and the representations of the two bonding mode extremes [(C) π-complex and (D) metallacyclopropane].

(1) (a) Dartmouth College. (b) University of Delaware.

(2) Love, R. A.; Koetzle, T. F.; Williams, G. J. B.; Andrews, L. C.; Bau, R. *Inorg. Chem.* **1975,** *14,* 2653 and references therein.

(3) See, for example: Parshall, G. W. *Homogeneous Catalysis*; Wiley-Interscience: New York, 1980. Collman, J. P.; Hegedus, L. S.; Norton, J. R.; Finke, R. *Principles and Applications of Organotransition Metal Chemistry*, 2nd ed.; University Science Books: Mill Valley, CA, 1987. Elschenbroich, C.; Salzer, A. *Organometallchemie*, Teubner: Stuttgart, 1986.

(4) (a) Dewar, M. J. S. *Bull. Soc. Chim. Fr.* **1951,** *18,* C79. (b) Chatt, J.; Duncanson, L. A. *J. Chem. Soc.* **1953,** 2339.

(5) (a) Albright, T. A.; Hoffmann, R.; Thibeault, J. C.; Thorn, D. L. *J. Am. Chem. Soc.* **1979,** *101,* 3801. (b) Mingos, D. M. P. In *Comprehensive Organometallic Chemistry*; Wilkinson, G., Abel, E., Stone, F. G. A., Eds.; Pergamon: Oxford, U.K., 1983; Vol. 3, Chapter 19, p 1. (c) Faller, J. W. *Adv. Organomet. Chem.* **1977,** *16,* 211. (d) Cotton, F. A. In *Dynamic Nuclear Magnetic Resonance*; Jackman, L. M., Cotton, F. A., Eds.; Academic Press: New York, 1975; p 377. (e) Mann, B. L. *Comprehensive Organometallic Chemistry*; Wilkinson, G., Abel, E., Stone, F. G. A., Eds.; Pergamon: Oxford, U.K., 1983; Vol. 3, Chapter 20, p 89.

0276-7333/93/2312-3102$04.00/0

metal d to olefin π^* interaction (Figure 1B) and its variation with the rotational conformation of the olefin with respect to the metal–olefin axis that is found to be responsible for most barriers to propeller rotation.[5a] In cases involving olefins ligated to d^6 ML_5 fragments, in which there are two degenerate metal d orbitals available for π back-bonding, and therefore a cylindrically symmetric back-bonding interaction, an unfavorable interaction between a filled metal d orbital and the filled olefin π bonding orbital, or some steric interaction, is usually found to be responsible for the observed barrier.[5a]

For complexes in which the olefin has electronegative substituents, significant π-back-bonding character in the metal–olefin bond leads to increased pyramidalization at the carbon atoms such that these metal–olefin complexes are generally referred to as metallacyclopropanes rather than as π complexes (see Figures 1C and 1D). Hoffmann and co-workers have emphasized that the bonding descriptions for these two types of interactions are of course identical; they are simply two extremes of a continuum of bonding possible within the Dewar–Chatt–Duncanson model of transition metal–olefin bonding.[5a] It should be noted that in the case of ligated C_2F_4, pyramidalization is a result not simply of electron-withdrawing F substituents increasing the π-back-bonding component but also because the energy of the olefin π^* orbital is lowered to give a better energy match with the metal d orbitals[6] and because repulsive interactions between occupied p orbitals on the F atoms and the C=C π-bond electrons are reduced.[7]

Higher barriers to propeller rotation are generally found in those complexes bearing electronegative substituents on the olefin,[5e,8] and this is usually ascribed to an increase in the π-back-bonding component of the metal–olefin interaction.[5] Since such compounds also possess metallacyclopropane structures, observation of this structural feature is often thought to imply automatically a high barrier to rotation. For example, the observation of conformationally static behavior on the NMR time scale in many d^8 and d^{10} tetrafluoroethylene complexes[8] has led to the assumption that propeller rotation of C_2F_4 ligands should invariably have high activation barriers. The olefin complex $[RhCp(C_2H_4)(C_2F_4)]$ (1) is a paradigm that allows

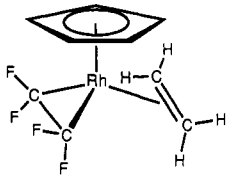

1

comparison between C_2H_4 and C_2F_4 ligands within the same molecule. While the C_2H_4 ligand rotates fast on the NMR time scale ($\Delta G^* = 56.9 \pm 2.5$ kJ mol^{-1}), the C_2F_4 ligand, which has all the structural attributes (see below) of a metallacyclopropane,[9] is not observed to undergo propeller rotation on the NMR time scale up to 100 °C, at which point the complex decomposes.[10]

The prediction that minimum activation barriers to olefin rotation should be found in complexes in which the olefin is bound to a d^6 ML_5 fragment, or an isolobal analogue,[5a] led us to speculate whether a demonstrably metallacyclopropane type structure could be found which would also exhibit the predicted low barrier to propeller rotation. Prior to our preliminary communication,[11] no measurements of activation free energies for propeller rotation of C_2F_4 ligands had been made. Indeed, only one reference to an apparently low barrier to C_2F_4 rotation has been made for the complex $[Ru_2Cp_2(\mu\text{-}CO)(\mu\text{-}CH_2)(CO)(C_2F_4)]$ (2)[12] but no further details have appeared. A

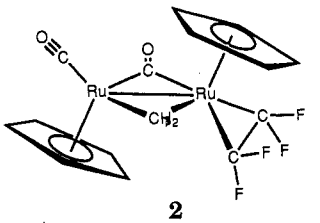

2

low barrier, unexpected in a d^8 complex,[5a] was implied by reports of the 56-MHz ^{19}F-NMR spectrum of $[Rh(acac)(C_2H_4)(C_2F_4)]$, for which a single chemical shift for all four F atoms was reported.[13] Since the ground state structure should have two fluorine environments this observation was suggestive of facile propeller rotation. We have shown subsequently that this is an unfortunate effect of the relatively low dispersion obtained at 56 MHz; the 282 MHz ^{19}F-NMR spectrum of this compound reveals a relatively small chemical shift difference for the two sets of symmetrically inequivalent ^{19}F environments (1.0 ppm in $CDCl_3$) and a clearly resolved AA'BB'X pattern (X = ^{103}Rh),[11] consistent with a conformationally static structure, and thus the relatively high barrier to propeller rotation expected[5a] for a d^8 complex. A small chemical shift difference is probably also the reason for the single F environment reported for the dipivalomethane analogue of this acac complex.[14]

In this paper we report the full details on the synthesis, characterization, and measurement of unprecedentedly low activation barriers to propeller rotation of η^2-tetrafluoroethylene ligands in a series of d^6 ruthenium complexes.

Experimental Section

General Considerations. Infrared spectra were recorded on a Bio-Rad Digilab FTS-40 FTIR spectrophotometer. ^{1}H (300 MHz), ^{13}C{^{1}H} (75 MHz), ^{31}P{^{1}H} (121 MHz), and ^{19}F{^{31}P} (282 MHz) NMR spectra were recorded on a Varian Associates XL-300 spectrometer at 25 °C unless otherwise noted. All ^{19}F-NMR shifts were recorded as ppm upfield from $CFCl_3$, while ^{1}H and ^{13}C{^{1}H} shifts were recorded as ppm downfield from tetramethylsilane. Chemical shifts for ^{31}P{^{1}H} were recorded as ppm downfield from 85% H_3PO_4 using the internal frequency lock of the spectrometer. All variable temperature spectra were recorded on a Varian Associates XL-300 spectrometer. The probe was calibrated at various temperatures by using samples of methanol (low temperature)[15] and ethylene glycol (high temperature).[16]

(6) Tolman, C. A. *J. Am. Chem. Soc.* **1974**, *96*, 2780.
(7) (a) Wang, S. Y.; Borden, W. T. *J. Am. Chem. Soc.* **1989**, *111*, 7282. (b) Getty, S. J.; Borden, W. T. *J. Am. Chem. Soc.* **1991**, *113*, 4334.
(8) Hughes, R. P. *Adv. Organomet. Chem.* **1990**, *31*, 183, and references therein.
(9) Guggenberger, L. J.; Cramer, R. *J. Am. Chem. Soc.* **1972**, *94*, 3779.
(10) Cramer, R.; Kline, J. B.; Roberts, J. D. *J. Am. Chem. Soc.* **1969**, *91*, 2519.
(11) Curnow, O. J.; Hughes, R. P.; Rheingold, A. L. *J. Am. Chem. Soc.* **1992**, *114*, 3153.
(12) Howard, J. A. K.; Knox, S. A. R.; Terrill, N. J.; Yates, M. I. *J. Chem. Soc., Chem. Commun.* **1989**, 640.
(13) Parshall, G. W.; Jones, F. W. *J. Am. Chem. Soc.* **1965**, *87*, 5356.
(14) Jarvis, A. C.; Kemmitt, R. D. W. *J. Organomet. Chem.* **1974**, *81*, 415.
(15) Van-Geet, A. L. *Anal. Chem.* **1968**, *40*, 2227.
(16) Piccini-Leopardi, C.; Fabre, A.; Reisse, J. *Org. Magn. Reson.* **1976**, *8*, 233.

Microanalyses were done at Spang Microanalytical Laboratory, Eagle Harbor, MI.

All solvents were obtained from Fisher Scientific, saturated with dinitrogen, and distilled over one of a variety of drying agents: THF, toluene, and diethyl ether from Na/benzophenone; CH_2Cl_2 and petroleum ether from CaH_2. All reactions were run in oven-dried glassware with the use of conventional Schlenk techniques under an atmosphere of dinitrogen that was deoxygenated over BASF catalyst and dried with Aquasorb, or in a Vacuum Atmospheres drybox equipped with a HE-492 gas purification system.

$RuCl_3 \cdot 3H_2O$ was obtained from Johnson Matthey Aesar/Alfa, tetrafluoroethylene was from PCR research chemicals, pentamethylcyclopentadiene was from Strem Chemicals, all deuterated solvents were from ISOTEC Inc., carbon monoxide was obtained from Air Products, and all other chemicals were from Aldrich Chemical Co. Inc. The Tl^+ salts were prepared by reaction of TlOEt (Aldrich) with the corresponding acid in hexane solution and filtering off the resultant product, which was used immediately. $[RuCp^*Cl]_4$ was prepared by the literature procedure.[17]

NMR simulations and line shape analyses were carried out using the DNMR program,[18] and ΔG^* values were calculated using the Eyring equation.[19]

$[RuCp^*(C_2F_4)Cl]_2$ (3). $[RuCp^*Cl]_4$ (0.19 g, 0.17 mol) was dissolved in CH_2Cl_2 (20 mL), and the solution was cooled to −78 °C. Tetrafluoroethylene was bubbled through the solution slowly as it was allowed to warm to ambient temperature, whereupon orange microcrystals of **3** formed. The crystals were collected by filtration and washed with toluene and diethyl ether to give 0.24 g (95% yield) of product: X-ray crystallographic quality crystals were obtained by slow cooling of a warm CH_2Cl_2 solution. Anal. Calcd for $C_{24}H_{30}Cl_2F_8Ru_2$: C, 38.77; H, 4.03. Found: C, 39.00; H, 4.13. Poor solubility precluded satisfactory NMR spectra.

$[RuCp^*(C_2F_4)$(pentane-2,4-dionato)$]$ (4a). Dimer **3** (0.104 g, 0.279 mmol of Ru) was dissolved in THF (50 mL), and thallium acetylacetonate (0.091 g, 0.300 mmol) was added. After stirring for 2 h, the solution was red-orange and a gray precipitate of TlCl had formed. The solution was then filtered through Celite. Removal of solvent in vacuo and crystallization from THF/petroleum ether gave **4a** as orange crystals (0.113 g, 93% yield): ^1H NMR (C_6D_6) δ 4.99 (s, 1H, CH), 1.73 (s, 6H, acac CH_3), 1.31 (s, 15H, Cp*); ^{19}F NMR (toluene-d_8, −35 °C, shifts relative to $CFCl_3$) δ −123.08 (m, 2F), −133.62 (m, 2F), $J_{AB} = J_{CD} = 140$ Hz, $J_{AD} = J_{BC} = -52.0$ Hz, $J_{AC} = 7.7$ Hz, $J_{BD} = 2.2$ Hz; $^{13}C\{^1H\}$ NMR ($CDCl_3$) δ 187.5 (acac CO), 124.2 (t, $J_{CF} = 325.5$ Hz, C_2F_4), 102.2 (CH), 100.7 ($C_5(CH_3)_5$), 27.9 (acac CH_3), 8.9 ($C_5(CH_3)_5$).

$[RuCp^*(C_2F_4)$(1,1,1-trifluoropentane-2,4-dionato)$]$ (4b). Dimer **3** (0.104 g, 0.279 mmol of Ru) was dissolved in THF (50 mL), and thallium trifluoroacetylacetonate (0.099 g, 0.279 mmol) was added. After overnight stirring, the solution was yellow and a gray precipitate of TlCl had formed. The solution was then filtered through Celite. Removal of solvent in vacuo and crystallization from THF/petroleum ether gave **4b** as an orange solid (0.107 g, 78% yield): ^1H NMR (C_6D_6) δ 5.46 (q, $^4J_{HF} = 0.4$ Hz, 1H, CH), 1.53 (s, 3H, CH_3), 1.21 (s, 15H, Cp*); ^{19}F NMR (toluene-d_8, −50 °C) δ −77.85 (s, CF_3), −122.81 (dd, F_B), −125.84 (dd, F_D), −134.10 (dd, F_C), −136.07 (dd, F_A), $J_{AB} = 141.3$ Hz, $J_{AC} = 0.0$ Hz, $J_{AD} = -53.5$ Hz, $J_{BC} = -54.3$ Hz, $J_{BD} \sim 0$ Hz, $J_{CD} = 136.6$ Hz. Anal. Calcd for $C_{17}H_{19}F_7O_2Ru$: C, 41.72; H, 3.91. Found: C, 41.53; H, 4.01.

$[RuCp^*(C_2F_4)$(2,6-dimethylheptane-3,5-dionato)$]$ (4c). Dimer **3** (0.1 g, 0.279 mmol of Ru) was dissolved in THF (15 mL) and the thallium dimethylheptanedionato salt (0.096 g, 0.27 mmol) added. After stirring for 12 h, the solution was red-orange and a gray precipitate of TlCl had formed. The solution was then filtered through Celite. Removal of solvent in vacuo and recrystallization from THF/petroleum ether gave the yellow solid **4c** (0.06 g, 45% yield): ^1H NMR (toluene-d_8) δ 5.13 (s, 1H, CH), 2.21 (septet, $J = 6.8$ Hz, 2H, $CH(CH_3)_2$), 1.35 (s, 15H, Cp*), 1.07 (d, $J = 6.8$ Hz, 6H, $CH(CH_3)_2$), 1.01 (d, $J = 6.8$ Hz, 6H, $CH(CH_3)_2$); ^{19}F NMR (toluene-d_8, −50 °C) δ −134.8 (m, 2F), −123.1 (m, 2F), $J_{AB} = J_{CD} = 140$ Hz, $J_{AD} = J_{BC} = -52$ Hz, $J_{AC} = 6$ Hz, $J_{BD} = 2$ Hz. Anal. Calcd for $C_{21}H_{30}F_4O_2Ru$: C, 50.09; H, 6.31. Found: C, 49.76; H, 6.35.

$[RuCp^*(C_2F_4)(PMe_3)Cl]$ (5a). A solution of the dimer **3** (0.0216 g, 0.0581 mmol of Ru) and PMe_3 (0.2 mL, 1.90 mmol) in CH_2Cl_2 (25 mL) was stirred overnight, resulting in a color change from orange to yellow. The solvent and excess PMe_3 were then removed in vacuo. Crystallization from CH_2Cl_2/petroleum ether yielded 0.0251 g (96% yield) of yellow product: ^1H NMR (C_6D_6) δ 1.41 (d, $J_{HP} = 1.5$ Hz, 15H, Cp*), 1.00 (d, $J_{HP} = 10.5$ Hz, 9H, PMe_3); ^{19}F NMR (C_6D_6) δ −124.2 (ddd, 1F, F_c), −122.0 (dddd, 1F, F_b), −118.6 (ddd, 1F, F_d), −115.5 (dddd, 1F, F_a), $J_{AB} = 157.1$ Hz, $J_{AC} = 9.7$ Hz, $J_{AD} = -44.9$ Hz, $J_{BC} = -49.0$ Hz, $J_{BD} = 4.3$ Hz, $J_{CD} = 146.7$ Hz, $J_{PFa} = 73.7$ Hz, $J_{PFb} = 5.7$ Hz; $^{31}P\{^1H\}$ NMR (C_6D_6) δ 14.03 (dd, $J_{PFa} = 73.7$ Hz, $J_{PFb} = 5.7$ Hz, PMe_3). Anal. Calcd for $C_{15}H_{24}ClF_4PRu$: C, 40.23; H, 5.40. Found: C, 39.77; H, 5.61.

$[RuCp^*(C_2F_4)\{P(OMe)_3\}Cl]$ (5b). A solution of **3** (0.2161 g, 0.58 mmol of Ru) and $P(OMe)_3$ (0.7 mL, 6.0 mmol) in THF (30 mL) was stirred overnight, resulting in a color change from orange to yellow. The solvent and excess $P(OMe)_3$ were then removed in vacuo, and the product was dissolved in diethyl ether and filtered through Celite. Removal of solvent in vacuo yielded 0.274 g (95% yield) of yellow powder: ^1H NMR (C_6D_6) δ 3.41 (d, $^3J_{PH} = 10.6$ Hz, 9H, $P(OMe)_3$), 1.54 (d, $^4J_{PH} = 2.4$ Hz, 15H, Cp*); ^{19}F NMR (C_6D_6) δ −108.1 (dddd, 1F, F_a), −119.2 (dd, 1F, F_d), −120.9 (dd, 1F, F_b), −122.6 (ddd, 1F, F_c), $J_{AB} = 153.6$ Hz, $J_{AC} = 6.3$ Hz, $J_{AD} = -46.8$ Hz, $J_{BC} = -50.2$ Hz, $J_{BD} \sim 0$ Hz, $J_{CD} = 144.6$ Hz, $J_{PFa} = 79.3$ Hz; $^{31}P\{^1H\}$ NMR (C_6D_6) δ 134.5 (d, $J_{PFa} = 79.3$ Hz, $P(OMe)_3$). Anal. Calcd for $C_{15}H_{24}ClF_4O_3PRu$: C, 36.33; H, 4.88. Found: C, 36.39; H, 5.00.

$[RuCp^*(C_2F_4)$(pyridine)Cl$]$ (5c). Dimer **3** (0.1 g, 0.013 mmol) and pyridine (3 mL, 12.3 mmol) were dissolved in THF (20 mL). After stirring for 24 h, the solution was orange. The solvent and excess pyridine were then removed in vacuo to give an orange solid which was recrystallized from THF/petroleum ether to give the product (0.52 g, 88% yield): ^1H NMR (acetone-d_6) δ 8.84 (d, 2H, py), 7.93 (tt, 1H, py), 7.43 (td, 2H, py), 1.56 (s, 15H, Cp*); ^{19}F NMR ($CDCl_3$) δ −117 (ddd, 1F, F_A), −125 (m, 2F, $F_{B,C}$), −127 (dd, 1F, F_D). Spectral overlap prevented detailed analysis of the coupling constants. Anal. Calcd for $C_{17}H_{20}ClF_4NRu$: C, 45.30; H, 4.48; N, 3.11. Found: C, 44.90; H, 4.57; N, 2.98.

$[RuCp^*(C_2F_4)(t$-BuNC)Cl$]$ (5d): Dimer **3** (0.061 g, 0.163 mmol of Ru) and *t*-BuNC (0.11 mL, 1.0 mmol) were dissolved in THF (30 mL). After stirring for 12 h, the solution was yellow. The solvent and excess *t*-BuNC were then removed in vacuo to give a yellow solid which was recrystallized from THF/petroleum ether to give the product (0.065 g, 88% yield): IR (CH_2Cl_2) ν_{NC} 2176 cm^{-1}; ^1H NMR (C_6D_6) δ 1.56 (s, 15H, Cp*), 0.91 (s, 9H, *t*-Bu); ^{19}F NMR (toluene-d_8, −20 °C) δ −109.54 (ddd, F_A), −119.50 (dd, F_B), −123.80 (ddd, F_C), −125.34 (dd, F_D), $J_{AB} = 140.8$ Hz, $J_{AC} = 4.2$ Hz, $J_{AD} = -48.6$ Hz, $J_{BC} = -50.3$ Hz, $J_{BD} = 0$ Hz, $J_{CD} = 142.4$ Hz. Anal. Calcd for $C_{17}H_{24}ClF_4NRu$: C, 44.89; H, 5.32; N, 3.08. Found: C, 45.57; H, 5.78; N, 3.59. These were the best analytical data that we could obtain on this compound.

$[RuCp^*(C_2F_4)$(8-hydroxyquinolinato)$]$ (6a). Dimer **3** (0.1 g, 0.267 mmol of Ru) was dissolved in THF (15 mL) and then thallium hydroxyquinolate salt (0.093 g, 0.268 mmol) added. After stirring for 4 h, the solution was orange-brown and a gray precipitate of TlCl had formed. The solution was then filtered through Celite. Removal of solvent in vacuo and recrystallization from THF/petroleum ether gave yellow crystals of product **6a** (0.015 g, 12% yield): ^1H NMR ($CDCl_3$) δ 1.58 (s, 15H, Cp*), 8.18 (d, 1H), 7.98 (dd, 1H), 6.72 (dd, 1H), 7.07 (dd, 1H), 7.20 (q, 1H),

(17) (a) Fagan, P. J.; Ward, M. D.; Caspar, J. C.; Krusic, P. J. *J. Am. Chem. Soc.* **1988**, *110*, 2981. (b) Fagan, P. J.; Ward, M. D.; Calabrese, J. C. *J. Am. Chem. Soc.* **1989**, *111*, 1698.

(18) The original version of the dynamic NMR simulation program was written by D. A. Kleier and G. Binsch: *J. Magn. Reson.* **1970**, *3*, 146–160; Program 165, Quantum Chemistry Program Exchange, Indiana University. Modifications are described in: Bushweller, C. H.; Bhat, G.; Lentendre, L. J.; Brunelle, J. A.; Bilofsky, H. S.; Ruben, H.; Templeton, D. H.; Zalkin, A. *J. Am. Chem. Soc.* **1975**, *97*, 65–73.

(19) Eyring, H. *Chem. Rev.* **1935**, *17*, 65–77.

Table I. Data for Crystallographic Determination of $[RuCp^*(C_2F_4)Cl]_2$ (3)

	(a) Crystal Parameters		
formula	$C_{24}H_{30}Cl_2F_8Ru_2$	V, Å^3	1308.3(5)
fw	743.5	Z	2
cryst syst	monoclinic	cryst dimens, mm	0.10 × 0.30 × 0.60
space group	$P2_1/n$	cryst color	orange-red
a, Å	8.059(2)	D(calc), g cm^{-3}	1.887
b, Å	20.504(6)	μ(Mo Kα), cm^{-1}	14.28
c, Å	8.830(1)	temp, K	298
β, deg	116.28(1)	T(max)/T(min)	0.8016
	(b) Data Collection		
diffractometer	Siemens P4	no. of rflns collected	3300
monochromator	graphite	no. of indpt rflns	3013
radiation (λ, Å)	Mo Kα (0.710 73)	no. of indpt obsvd rflns $F_o \geq n\sigma(F_o)$ (n = 0)	2461
2θ scan range, deg	4.0–55.0	no. of std rflns	3 std/197 rflns
data collcd (h,k,l)	±10,±26,±11	var in stds, %	<2
	(c) Refinement		
$R(F)$, %	4.56	$\Delta(\rho)$, e Å^{-3}	0.54
$R(wF)$, %	5.30	N_o/N_v	18.4
Δ/σ(max)	0.002	GOF	1.17

7.28 (dd, 1H); ^{19}F NMR ($CDCl_3$): δ −136.4 (dd, 1F, F_a), −129.1 (dd, 2F, F_b), −124.1 (dd, 1F, F_c), −121.6 (dd, 1F, F_d), J_{AB} = 146.8 Hz, J_{AD} = −49.8 Hz, J_{BC} = −50.2 Hz, J_{CD} = 139.1 Hz. Anal. Calcd for $C_{21}H_{21}F_4NORu$: C, 52.50; H, 4.41; N, 2.92. Found: C, 52.80; H, 4.48; N, 2.71.

[RuCp*(C_2F_4)(8-hydroxyquinaldinato)] (6b). Dimer **3** (0.1 g, 0.267 mmol of Ru) was dissolved in THF (15 mL) and the thallium hydroxyquinaldinate salt (0.1 g, 0.268 mmol) added. After stirring for 12 h, the solution was red-orange and a gray precipitate of TlCl had formed. The solution was then filtered through Celite. After removal of solvent in vacuo and recrystallization from THF/petroleum ether, 0.06 g (45% yield) of yellow solid **6b** was obtained: ^{1}H NMR (acetone-d_6) δ 8.04 (d), 7.37 (d), 7.20 (t), 6.95 (d), 6.73 (dd), 2.90 (s, 15H, Cp*), 1.59 (s, 3H, Me); ^{19}F NMR ($CDCl_3$) δ −134.8 (dd, 1F, F_a), −127.0 (dd, 1F, F_d), −121.5 (dd, 1F, F_c), −119.0 (dd, 1F, F_b), J_{AB} = 146.0 Hz, J_{AC} = 0 Hz, J_{AD} = −47.9 Hz, J_{BC} = −48.6 Hz, J_{BD} = 0 Hz, J_{CD} = 147.8 Hz. Anal. Calcd for $C_{22}H_{23}ClF_4NORu$: C, 53.40; H, 4.69; N, 2.83. Found: C, 53.49; H, 4.70; N, 2.60.

Reaction of $[RuCp^*(C_2F_4)Cl]_2$ with CO. $[RuCp^*(C_2F_4)Cl]_2$ (0.073 g, 0.20 mmol of Ru) was dissolved in THF (30 mL) in a Fischer-Porter vessel which was then pressurized to 20 psi with CO and stirred overnight. Removal of solvent in vacuo and extraction with diethyl ether gave a yellow compound which was identified spectroscopically as $[RuCp^*(CO)_2Cl]$ by comparison with the literature data.[20]

X-ray Crystallographic Study of $[RuCp^*Cl(C_2F_4)]_2$ (3). A crystal suitable for X-ray structural determination was mounted on a glass fiber with epoxy cement. Crystal, data collection, and refinement parameters are collected in Table I. The unit-cell parameters were obtained from the least squares fit of 25 reflections (20° ≤ 2θ ≤ 25°). The systematic absences in the diffraction data uniquely established the space group as $P2_1/n$. The semiempirical absorption correction program XABS was applied to the data set.[21]

The structure was solved by direct methods which located the Ru atom. The remaining non-hydrogen atoms were located through subsequent difference Fourier syntheses. All hydrogen atoms were included as idealized isotropic contributions (d_{CH} = 0.960 Å, U = 1.2U for attached C). All non-hydrogen atoms were refined with anisotropic thermal parameters. The asymmetric unit contains one independent half-molecule which resides on a crystallographic inversion center. All software and the sources of the scattering factors are contained in the SHELXTLPLUS-(4.2) program library.[22]

(20) Bailey, N. A.; Radford, S. R.; Sanderson, J. A.; Tabatabaian, K.; White, C.; Worthington, J. M. *J. Organomet. Chem.* **1978**, *154*, 343.
(21) Hope, H.; Moezzi, B. University of California—Davis, private communication to A.L.R.
(22) Sheldrick, G. Siemens XRD, Madison, WI.

Results and Discussion

Synthesis and Structure of $[RuCp^*(C_2F_4)(\mu\text{-}Cl)]_2$ (3). Tetrafluoroethylene reacts with the tetramer $[RuCp^*Cl]_4$ to form the chloro-bridged dimer $[RuCp^*(C_2F_4)Cl]_2$ (**3**) as orange microcrystals in high yield. Fagan

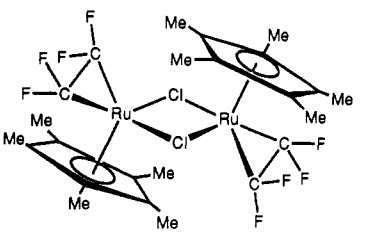

3

et al. recently prepared the ethylene analogue of **3** under 60 psi of C_2H_4 but were unable to obtain suitable crystals for an X-ray structural determination due to a lack of solubility.[23] The tetrafluoroethylene complex **3** is likewise quite insoluble, only dissolving slightly in warm THF or CH_2Cl_2. Koelle and co-workers were able to obtain a pentane soluble ethylene analogue of **3** by using the tetramethylethylcyclopentadienyl ligand rather than Cp* and were able to obtain an X-ray structure of this dimer $[Ru(C_5Me_4Et)(C_2H_4)Cl]_2$.[24]

The structure of **3** was confirmed by a single crystal X-ray diffraction study. An ORTEP plot is shown in Figure 2, positional parameters are collected in Table II, and selected bond distances and angles are listed in Table III. Like $[Ru(C_5Me_4Et)(C_2H_4)Cl]_2$,[24] dimer **3** exhibits a crystallographic inversion center, necessitating a planar Ru_2Cl_2 ring and a *trans* arrangement of the Cp* ligands (Figure 2). Similarly, the long Ru···Ru distance [3.797(9) Å] rules out any Ru—Ru bonding interaction. While the Ru—Cp*(centroid) distance in **3** is longer than that in $[Ru(C_5Me_4Et)(C_2H_4)Cl]_2$ [1.890(5) Å vs 1.815 Å], the average Ru—Cl distances are slightly shorter (2.45 Å vs 2.48 Å). The Cl ligands in **3** are on average slightly closer to the Cp* ligand, and the C—Ru—Cl angles are all 2–5 deg larger in **3** than those in $[Ru(C_5Me_4Et)(C_2H_4)Cl]_2$; this may be a consequence of steric interactions with the

(23) Fagan, P. J.; Mahoney, W. S.; Calabrese, J. C.; Williams, I. D. *Organometallics* **1990**, *9*, 1843.
(24) Koelle, U.; Kang, D.-S.; Englert, U. *J. Organomet. Chem.* **1991**, *420*, 227.

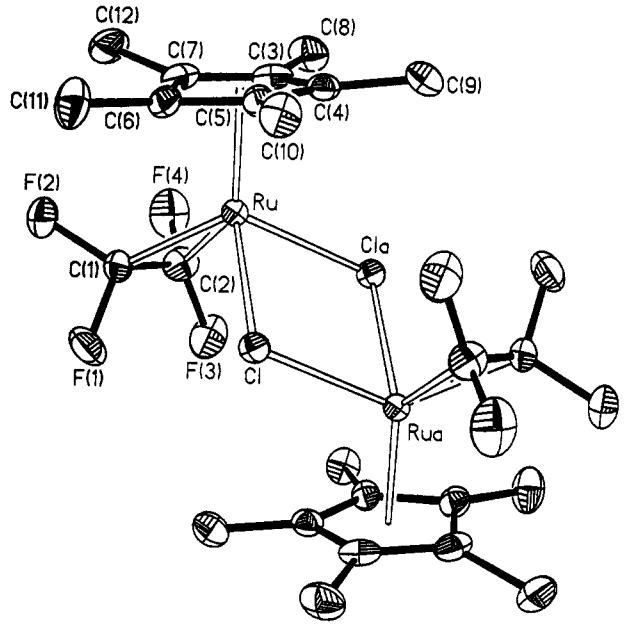

Figure 2. ORTEP plot of $[RuCp^*(C_2F_4)(Cl)]_2$ (**3**).

Table II. Atomic Coordinates (×10⁴) and Equivalent Isotropic Displacement Coefficients (Å² × 10³) for $[RuCp^*(C_2F_4)Cl]_2$ (3)

	x	y	z	U(eq)[a]
Ru	553(1)	9143(1)	4548(1)	23(1)
Cl	1296(1)	10290(1)	4286(1)	28(1)
F(1)	-463(6)	9579(2)	1008(4)	63(2)
F(2)	-23(5)	8536(2)	1221(4)	52(1)
F(3)	-3236(4)	9455(2)	1922(4)	66(1)
F(4)	-2770(5)	8408(2)	2249(4)	64(2)
C(1)	-462(7)	9057(2)	1966(6)	37(2)
C(2)	-1884(7)	8995(3)	2446(6)	41(2)
C(3)	1018(6)	8296(2)	6171(6)	37(2)
C(4)	2346(6)	8766(2)	7299(5)	31(2)
C(5)	3588(6)	8920(2)	6619(5)	30(2)
C(6)	3029(6)	8569(2)	5025(6)	33(2)
C(7)	1539(6)	8135(2)	4877(6)	38(2)
C(8)	-405(7)	7949(3)	6488(7)	49(2)
C(9)	2425(8)	8994(3)	8914(6)	47(2)
C(10)	5220(6)	9373(3)	7367(6)	42(2)
C(11)	4138(8)	8549(3)	4066(7)	55(2)
C(12)	904(9)	7554(2)	3701(7)	53(2)

[a] Equivalent isotropic U defined as one-third of the trace of the orthogonalized U_{ij} tensor.

slightly larger C_2F_4 ligand, although the Cp*—Ru—C angles are essentially the same {120.3(2) and 130.3(2)° in **3** versus 119.85 and 129.24° in $[Ru(C_5Me_4Et)(C_2H_4)Cl]_2$}. The olefin ligand and the two chloride ligands are twisted to essentially the same degree with respect to the Cp* ring in both **3** and $[Ru(C_5Me_4Et)(C_2H_4)Cl]_2$; the Cl—C—C—Cl torsion angle in **3** is 17.8°, while in $[Ru(C_5Me_4Et)(C_2H_4)Cl]_2$ it is 16.8°. As is to be expected for a metallacyclopropane structure, a longer olefin C=C bond is found in **3** than in the C_2H_4 complex [1.393(9) Å vs 1.369(9) Å] and the Ru—C distance is shorter [2.051(5) Å versus 2.194(4) Å]. Evaluation of the parameters used to define how much the substituents bend back (Table IV), as defined by Ittel and Ibers (Figure 3),[25] shows the $Ru(C_2F_4)$ unit to have a metallacyclopropane structure essentially identical to those previously defined for $[RuCp^*(acac)(C_2F_4)]$[11] and $[RhCp(C_2H_4)(C_2F_4)]$.[9]

Reaction of $[RuCp^*(C_2F_4)Cl]_2$ (3) with Carbon Monoxide. There was no observable reaction of **3** with CO at 1 atm under ambient conditions, but prolonged reaction under CO pressure resulted only in displacement of the C_2F_4 ligand. Koelle *et al.* reported that the reaction of $[Ru(C_5Me_4Et)(C_2H_4)Cl]_2$ with CO first gives C_2H_4 substitution to afford the intermediates $[Ru(C_5Me_4Et)(CO)Cl]_2$ (two structural isomers) and then the final product $[Ru(C_5Me_4Et)(CO)_2Cl]$.[24] The compound $[Ru(C_5Me_4Et)(C_2H_4)(CO)Cl]$ was not observed. Due to the poor solubility of the dimer **3**, it is not possible to build up a significant amount of any intermediates and only $RuCp^*(CO)_2Cl$ was observed as the final product in our reaction.

Synthesis and NMR Studies of Monomeric C_2F_4 Complexes of Ruthenium. The poor solubility of **3** precluded a study of its variable temperature NMR spectra, but the synthesis of a variety of mononuclear derivatives circumvented this problem. Treatment of a suspension of **3** in dichloromethane or THF with the thallium salt of a β-diketonate ligand afforded the mononuclear derivatives **4a–c**. The molecular structure of the acac complex **4a** has been published previously,[11] and key structural comparisons to that of **3** are provided in Table IV. At low temperatures the ^{19}F NMR spectrum of **4a** exhibited the expected two resonances for the symmetry

Table III. Selected Intramolecular Bond Distances and Angles for $[RuCp^*(C_2F_4)Cl]_2$ (3)

(a) Bond Distances (Å)			
Ru–RuA	3.797(9)	Ru–C(1)	2.061(5)
Ru–C(2)	2.041(4)	Ru–Cl	2.462(1)
Ru–CNT[a]	1.890(5)	Ru–ClA	2.448(1)
C(1)–C(2)	1.393(9)	C(1)–F(1)	1.364(6)
C(1)–F(2)	1.380(6)	C(2)–F(3)	1.358(6)
C(2)–F(4)	1.371(6)		
(b) Bond Angles (deg)			
Cl–Ru–CNT[a]	123.5(1)	ClA–Ru–CNT[a]	116.0(2)
C(1)–Ru–CNT[a]	120.3(2)	C(2)–Ru–CNT[a]	130.3(2)
Cl–Ru–ClA	78.7(1)	Cl–Ru–C(1)	88.4(1)
Cl–Ru–C(2)	103.5(1)	C(1)–Ru–ClA	119.2(2)
C(2)–Ru–ClA	86.2(2)	C(1)–Ru–C(2)	39.7(2)
F(1)–C(1)–F(2)	103.9(5)	F(1)–C(1)–C(2)	119.1(4)
F(2)–C(1)–C(2)	119.6(4)	F(3)–C(2)–F(4)	105.8(4)
F(3)–C(2)–C(1)	118.5(5)	F(4)–C(2)–C(1)	119.6(5)
Ru–C(1)–F(1)	120.7(3)	Ru–C(1)–F(2)	122.3(3)
Ru–C(2)–F(3)	120.7(3)	Ru–C(2)–F(4)	118.9(3)

[a] CNT = Centroid of atoms C(3) to C(7).

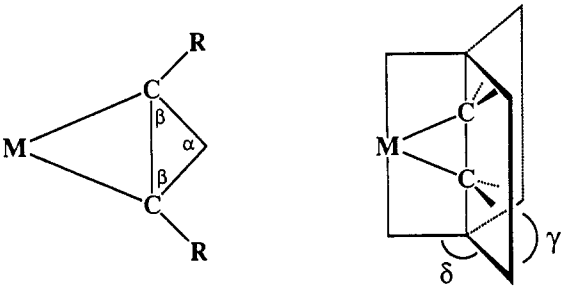

Figure 3. Angles used to define the degree with which olefin substituents are bent back.[25]

Table IV. Bond Distances and Angles (See Figure 3) Defining the M–C_2F_4 Structure in Selected C_2F_4 Complexes

	$[RuCp^*(C_2F_4)(acac)]$ (**4a**)[11]	$[RuCp^*(C_2F_4)Cl]_2$ (**3**)	$[RhCp(C_2H_4)(C_2F_4)]$ (**1**)[9]
d(C–F) (Å)	1.349(7)	1.368(6)	1.351(3)
d(C–M) (Å)	2.047(6)	2.051(4)	2.024(2)
d(C–C) (Å)	1.395(9)	1.393(9)	1.405(7)
α (deg)	73.9	73.7	74.3
β (deg)	53.0	53.1	52.8
δ (deg)	114.5	114.5	114.3
γ (deg)	131.0	131.0	131.4

(25) Ittel, S. D.; Ibers, J. A. *Adv. Organomet. Chem.* **1976**, *14*, 33.

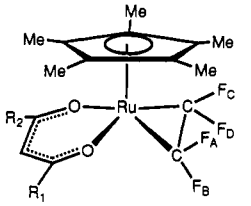

4 a. $R_1 = R_2 = CH_3$ ($F_A \equiv F_C$; $F_B \equiv F_D$)
b. $R_1 = CH_3$; $R_2 = CF_3$
c. $R_1 = R_2 = i\text{-}Pr$ ($F_A \equiv F_C$; $F_B \equiv F_D$)

inequivalent fluorine sites; F_A and F_C are proximal, and F_B and F_D are distal, to the Cp* ring. A variable temperature ^{19}F-NMR study of complex **4a** revealed a two resonance to one resonance coalescence with $\Delta G^{\ddagger} = 55 \pm 2$ kJ mol^{-1}. Proximal and distal environments could be interconverted either by propeller rotation of the C_2F_4 ligand or by an olefin dissociation/recombination mechanism. To rule out the latter pathway for the scrambling of the F environments, the corresponding trifluoroacetylacetonato (tfacac) complex **4b** was prepared and its variable temperature ^{19}F-NMR spectra were studied. The two different substituents on the β-diketonate ligand lower the symmetry of the molecule, making all four fluorine environments symmetrically inequivalent in the ground state structure. A dissociation/recombination pathway would interconvert all environments randomly, but propeller rotation would only allow interchange of mutually *trans* fluorines (i.e. $F_a \rightarrow F_d$, $F_d \rightarrow F_a$ and $F_b \rightarrow F_c$, $F_c \rightarrow F_b$). Behavior consistent with olefin rotation was observed as the four resonances coalesced to two upon raising the temperature.[11] A figure depicting this variable temperature behavior can be found in ref 11.

In a pseudo-5-coordinate species such as **4**, propeller rotation of the olefin could also be coupled to a pseudorotation at the metal center, and factors related to the activation barrier for this pseudorotation could contribute to the overall free energy of activation. Such behavior has been observed in other 5-coordinate olefin complexes of general formula [Fe(CO)$_4$(olefin)],[26] in which the barrier to pseudorotation at the metal center is dependent on the barrier to propeller rotation of the olefin. Accordingly, we designed an experiment to confirm or exclude pseudorotation as contributing to the dynamic behavior of complexes **4**. Complex **4c** is an analogue of **4a** with proximal and distal fluorine environments, but with an added spectroscopic probe of diastereotopic methyl groups in the isopropyl substituents of the β-diketonate ligand. Pseudorotation at the metal center would interconvert diastereotopic methyl environments, but a simple olefin rotation would not. The variable temperature ^{19}F- and ^{1}H-NMR spectra of **4c** showed the expected two to one resonance coalescence of proximal and distal fluorines without any corresponding site exchange of the diastereotopic methyl groups within the isopropyl groups over the same temperature range, thus excluding a pseudorotation on the same time scale as olefin rotation. Therefore, the only remaining explanation for the observed site exchange of fluorine substituents is that of propeller rotation about the Ru–olefin axis, and we feel that the values of $\Delta G^{\ddagger}$ measured in our experiments (see below) are indeed representative of a pure olefin rotation, unsullied by contributions from other dynamic processes.

(26) Kruczynski, L.; LiShingMan, L. K. K.; Takats, J. *J. Am. Chem. Soc.* **1974**, *96*, 4006.

Table V. Activation Free Energies ($\Delta G^{\ddagger}$) for Propeller Rotation of the C_2F_4 Ligand in d^6 Ruthenium Complexes

complex	$\Delta G^{\ddagger}$ (kJ mol^{-1})
[RuCp*(C_2F_4)(acetylacetonato)] (**4a**)	55 ± 2
[RuCp*(C_2F_4)(trifluoroacetylacetonato)] (**4b**)	53 ± 3
[RuCp*(C_2F_4)(dimethylheptanedionato)] (**4c**)	56 ± 1
[RuCp*(C_2F_4)(PMe_3)Cl] (**5a**)	81 ± 2
[RuCp*(C_2F_4){$P(OMe)_3$}Cl] (**5b**)	68 ± 2
[RuCp*(C_2F_4)(*t*-BuNC)Cl] (**5d**)	59 ± 2
[RuCp*(C_2F_4)(hydroxyquinolinato)] (**6a**)	65 ● 3
[RuCp*(C_2F_4)(hydroxyquinaldinator)] (**6b**)	63 ± 2

Attempts to prepare the hexafluoroacetylacetonato analogue of complexes **4** resulted in an orange solid which exhibited ^{1}H NMR resonances at 5.97 (1H) and 1.07 ppm (15H, Cp*) and ^{19}F resonances at −77.2 ppm (s, 6F, CF_3) and a broad peak at −127 ppm (4F, C_2F_4), but the compound was thermally unstable with respect to loss of C_2F_4 and further data were not pursued.

Other mononuclear derivatives were prepared by bridge cleavage reactions of **3** with monodentate ligands. In contrast to the reaction of **3** with CO (*vide supra*) the corresponding reactions with excess PMe_3, $P(OMe)_3$, pyridine, or *t*-BuNC afforded the monomeric derivatives **5a–d**. All of these reactions are slow, with overnight

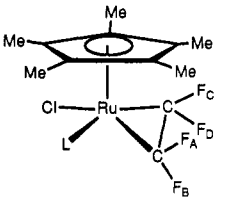

5 a. L = PMe_3
b. L = $P(OMe)_3$
c. L = pyridine
d. L = t-BuNC

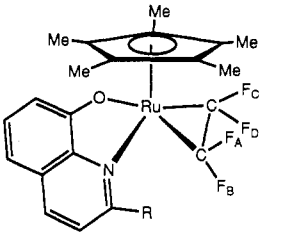

6 a. R = H
b. R = CH_3

stirring with a large excess of ligand being required, but the products are obtained in good yield, without problems involving displacement of C_2F_4. Two more unsymmetrical derivatives **6a,b** were prepared by reaction of **3** with the thallium salts of the appropriate hydroxyquinoline.

In general, the low temperature ^{19}F-NMR spectra of complexes **5** and **6** show four coupled multiplets in an AGMX pattern. Fluorine–fluorine coupling constants in all these compounds are consistent; the geminal couplings are in the range 135–155 Hz, the *trans* couplings 44–55 Hz, and the *cis* couplings 0–10 Hz. The phosphorus containing complexes **5a** and **5b** also display one large $^{3}J_{PF}$ coupling (73.7 and 79.3 Hz, respectively) and one small $^{3}J_{PF}$ coupling (5.7 and approximately 0 Hz, respectively). The strongly coupled F atom is assigned to the position *trans* to the phosphine, as this will have the P–Ru–C–F torsion angle closest to 180°, i.e. F_A in the line drawing.

Line shape analysis was used to simulate the observed ^{19}F-NMR spectra of complexes **4–6**, and values of $\Delta G^{\ddagger}$ for propeller rotation of the C_2F_4 ligands were calculated using the Eyring equation. Good data could not be obtained for the pyridine complex **5c** due to overlapping resonances and uncertainties in values of coupling constants. The measured activation free energies are collected in Table V. The symmetrical complexes **4** have the lowest values ($\Delta G^{\ddagger}$ = 53–56 kJ mol^{-1}); these activation barriers for C_2F_4 rotation are at the low end of those usually found for C_2H_4 rotation in d^8 and d^{10} complexes[5e] and are unprecedentedly low for C_2F_4. A simple rationale for the observed low

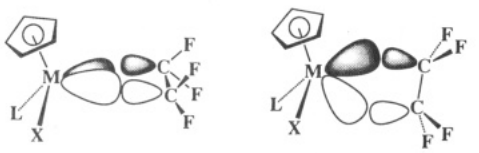

Figure 4. Overlap of the C_2F_4 π^* orbital with the frontier orbitals on the RuCp*(LX) fragment as the olefin undergoes propeller rotation.

barriers is found if one considers the RuCp*(LX) fragment, to a first approximation, to be a d^6 ML_5 fragment, in which case there are two filled, orthogonal, and degenerate d orbitals on the metal available for π back-bonding to the C_2F_4 ligand.[5a] In reality these orbitals will have neither the same spatial properties nor the same energy, but presumably the combination of orbital overlap properties and energy of these fragment MOs allows the parallel and perpendicular orientations of the C_2F_4 ligand (Figure 4) with respect to the Cp* plane to be close in energy and overlap, thus facilitating propeller rotation.[5a]

In the unsymmetrical derivatives **5** and **6**, somewhat higher barriers are found, with the strong σ-donor ligand PMe_3 derivative **5a** showing the highest activation barrier ($\Delta G^{\ddagger} = 81 \pm 2$ kJ mol^{-1}) of all the compounds investigated. By use of the weaker σ-donor ligand $P(OMe)_3$, the activation barrier is lowered to 68 ± 2 kJ mol^{-1} and is lowered even further with *t*-BuNC to 59 ± 2 kJ mol^{-1}. Thus, as with most olefin complexes, an increase in electron density on the metal leads to higher activation barriers for propeller rotation, which is usually attributed to an increase in the π-back-bonding character of the transition metal–olefin bond. Perhaps not unexpectedly, the mixed N-donor/O-donor combination in the hydroxyquinolinato derivative **6** gives barriers at the low end of this range, closer to those of compounds **4**, with two O-donors; the presence of the ortho CH_3 group in **6b** has no effect on the barrier compared to **6a**, implying that steric effects are minimal in this system. In the absence of steric effects and if the d orbitals on the metal shown in Figure 4 were truly degenerate, no change in the barrier to rotation would be expected. Detailed calculations on the effects of these ancillary ligands on the energies and polarization of these key orbitals is required before a more detailed rationale for these data can be achieved.

Conclusion

These observations confirm the prediction[5a] that olefin complexes containing electronegative substituents, and which have metallacyclopropane structures, will not necessarily have high barriers to propeller rotation of the olefin.

Acknowledgment. R.P.H. is grateful to the Air Force Office of Scientific Research and to the National Science Foundation for generous support, and to Johnson Matthey Aesar/Alfa for a generous loan of precious metal salts.

Supplementary Material Available: Tables of bond lengths, bond angles, anisotropic displacement coefficients, and H-atom coordinates and isotropic displacement coefficients for complex **3** (3 pages). Ordering information is given on any current masthead page.

OM9301546